

Separating Cloud and Drizzle Radar Moments during Precipitation Onset Using Doppler Spectra

EDWARD P. LUKE

Atmospheric Sciences Division, Brookhaven National Laboratory, Upton, New York

PAVLOS KOLLIAS

Department of Atmospheric and Oceanic Sciences, McGill University, Montreal, Quebec, Canada

(Manuscript received 24 October 2011, in final form 17 October 2012)

ABSTRACT

The retrieval of cloud, drizzle, and turbulence parameters using radar Doppler spectra is challenged by the convolution of microphysical and dynamical influences and the overall uncertainty introduced by turbulence. A new technique that utilizes recorded radar Doppler spectra from profiling cloud radars is presented here. The technique applies to areas in clouds where drizzle is initially produced by the autoconversion process and is detected by a positive skewness in the radar Doppler spectrum. Using the Gaussian-shape property of cloud Doppler spectra, the cloud-only radar Doppler spectrum is estimated and used to separate the cloud and drizzle contributions. Once separated, the cloud spectral peak can be used to retrieve vertical air motion and eddy dissipation rates, while the drizzle peak can be used to estimate the three radar moments of the drizzle particle size distribution. The technique works for nearly 50% of spectra found near cloud top, with efficacy diminishing to roughly 15% of spectra near cloud base. The approach has been tested on a large dataset collected in the Azores during the Atmospheric Radiation Measurement Program (ARM) Mobile Facility deployment on Graciosa Island from May 2009 through December 2010. Validation of the proposed technique is achieved using the cloud base as a natural boundary between radar Doppler spectra with and without cloud droplets. The retrieval algorithm has the potential to characterize the dynamical and microphysical conditions at cloud scale during the transition from cloud to precipitation. This has significant implications for improving the understanding of drizzle onset in liquid clouds and for improving model parameterization schemes of autoconversion of cloud water into drizzle.

1. Introduction

Advancing our understanding of the cloud-scale physical processes that affect cloud lifetime requires high-resolution measurements in clouds (Brenquier and Wood 2009). One area of great interest is the separation of cloud and drizzle microphysics and turbulence in warm clouds to shed light on precipitation initiation, including the role of aerosols and dynamics. Aircraft penetrations can provide detailed in situ measurements of these quantities; however, they are expensive, dimensionally challenged (1D flight track only) and have small sampling volumes. On the other hand, profiling cloud radar observations

(Kollias et al. 2007), complemented by other passive and active remote sensors, are continuously available from ground-based observational networks [the U.S. Department of Energy (DOE) Atmospheric Radiation Measurement Program (ARM) and the European Union (EU) CloudNet]. Although profiling cloud radar observations are not three dimensional, they do provide one additional dimension (vertical) but suffer from large uncertainties associated with the inversion of radar observables to microphysical and dynamical retrievals.

The potential of retrieving cloud and precipitation properties from Doppler spectra has been recognized since the early days of radar meteorology (Battan 1964; Rogers and Pilié 1962; Atlas et al. 1973). This assessment is based on the fact that in a vertically pointing mode, the observed Doppler velocity is related to the hydrometeor fall velocity. Thus, the range of observed Doppler velocities in the radar spectrum can be used to

Corresponding author address: Edward P. Luke, Atmospheric Sciences Division, Brookhaven National Laboratory, Bldg. 490D, Bell Ave., Upton, NY 11973.
E-mail: eluke@bnl.gov

infer the size range of hydrometeors in the sampling volume. It is also well known that small-scale air turbulence and volume-averaged vertical air motion within the radar sampling volume are the primary sources of uncertainty in retrieving cloud and precipitation microphysical information (Kollias et al. 2011a). These uncertainties could lead to errors up to 1 m s^{-1} (Atlas et al. 1973) in the retrieved vertical air motion and subsequently large errors in the retrieved particle size distribution. Since the early work of Atlas et al. (1973), several techniques have been proposed, developed, and tested for profiling radars operating over a wide range of frequencies (e.g., Hauser and Amayenc 1981; Gossard 1994; 1997; Frisch et al. 1995; Babb et al. 1999; Deng and Mace 2006; Delanoë et al. 2007). These techniques are based on iterative procedures that either use the Doppler spectrum moments or attempt to match a forward-modeled Doppler spectrum with the observed one, assuming a functional form for the particle size distribution. Furthermore, these techniques either have not accounted for the impact of turbulence on the observed spectrum shape and moments or have had limited information on how to correctly account for its impact. This is a direct outcome of these techniques being developed for radar Doppler spectra observed under Rayleigh scattering conditions, where the spectra do not contain features that facilitate the detection of the vertical air motion (Kollias et al. 2002).

How can we overcome these challenges using features of the Doppler spectrum? Not surprisingly, two of the most accurate techniques for quantifying the impact of turbulence utilize non-Rayleigh scattering signatures on the observed Doppler spectrum. These signatures enable the direct retrieval of the vertical air motion without the need for microphysical assumptions. The first technique utilizes the sensitivity of long wavelength wind profilers to coherent (Bragg) scattering and uses the Bragg spectral peak to directly measure air motion and spectral broadening due to turbulence (Wakasugi et al. 1986; Rogers et al. 1993; Williams et al. 1995). The second technique utilizes non-Rayleigh signatures from raindrops at 94 GHz (e.g., Lhermitte 1988; Kollias et al. 2002; Giangrande et al. 2010). Application of these two retrieval techniques in cloud research is restricted by the limited sensitivity of wind profilers to cloud and drizzle particles in the former and the need for large raindrops in the radar sampling volume in the latter. One could conclude that what is missing is a technique that works on millimeter wavelength radars (a required condition to detect small cloud droplets) and allows measurements of vertical air motion and turbulence broadening. Such measurements are routinely available in nonprecipitating clouds where the cloud droplets are

used as air tracers to determine the vertical air motion and turbulence broadening that can lead to estimates of the eddy dissipation rate (e.g., Kollias et al. 2001). However, this approach requires negligible fall velocity for the particles that contribute to the radar Doppler spectrum, and thus is not appropriate for radar volumes that contain larger particles (e.g., ice crystals or drizzle droplets) with nonnegligible fall velocity.

The concept of an “air motion tracer” in the radar resolution volume is shared by the Bragg scattering technique in wind profilers (inhomogeneities of the index of refraction do not have a terminal velocity) and the Rayleigh scattering technique in cloud radars (small liquid cloud droplets have negligible terminal velocity). One could assert that the Rayleigh scattering from cloud droplets is the equivalent “Bragg echo” used in clouds to directly measure the air motion and turbulence broadening of the radar Doppler spectrum. One of the reasons the Bragg scattering-based technique in wind profilers is successful is the fact that the Rayleigh hydrometeor scattering component is from raindrops that have significant fall velocity, and thus the two spectral peaks are often well separated in the recorded Doppler spectrum. It is relatively straightforward to exploit this spectral gap and to detect both peaks in the Doppler spectrum, thus retrieving both dynamical and microphysical parameters in precipitation (Williams et al. 2000). Such spectral gaps have also been observed between cloud peaks and drizzle or ice crystal peaks in millimeter wavelength radar, and they can be exploited in a similar manner (e.g., Shupe et al. 2004). However, because of the sensitivity of cloud radars to all particles in the radar sampling volume and the fact that small drizzle droplets and ice crystals have small terminal velocities, such spectral gaps are not frequently observed. Nevertheless, decomposing the observed radar Doppler spectrum into its cloud peak and drizzle/ice/precipitation peak has been the subject of past efforts (e.g., Gossard 1994; Babb et al. 1999; Luke et al. 2010).

Here, a new technique is described that extends the use of the cloud spectral peak as an air motion tracer in the presence of small drizzle particles and separates the cloud and drizzle returns in radar Doppler spectra. The technique is limited to areas in clouds where drizzle particles are initially produced and thus the radar reflectivity is still controlled by the cloud droplet distribution. The detection of drizzle particles under such conditions is based on the use of the radar Doppler spectrum skewness (e.g., Kollias et al. 2011a). The technique is applied to an extensive dataset of radar Doppler spectra collected by the W-band ARM Cloud Radar (WACR) during the recent U.S. DOE ARM Mobile Facility (AMF) deployment on Graciosa Island in the Azores. Key WACR operating parameters are

TABLE 1. Key operating parameters of the WACR.

Wavelength	3.154 mm
Pulse repetition frequency	10 000 Hz
Nyquist velocity	7.885 m s ⁻¹
No. of FFT bins	256
No. of spectral averages	80
Velocity resolution	0.0616 m s ⁻¹
Gate spacing	42.86 m
Integration time	2.048 s
Spectrum temporal spacing	4.096 (2.048) s*

* Longer temporal spacing applies to data used from 2009 when two interleaved radar modes were used. For data from 2010, only a single radar mode was used, and the shorter interval applies.

listed in Table 1. The spectral decomposition leads to the retrieval of vertical air motion, eddy dissipation rate, and drizzle particle radar moments. The technique is applicable to both unimodal and bimodal radar Doppler spectra. Detailed time–height retrievals and comparisons of the drizzle properties above and below the cloud base are presented to demonstrate the potential of the retrieval.

2. Methodology

The proposed method aims to quantitatively separate cloud and drizzle radar returns during precipitation onset conditions and to produce quantitative estimates of their Doppler moments. Precipitation onset (e.g., spectral broadening) conditions are defined as areas within clouds where the first small drizzle particles are produced. In radar Doppler spectrum representation, the first drizzle particles are detected as a small power spectral density enhancement at higher fall Doppler velocities. These small spectral density enhancements can be detected as a perturbation in the background cloud-only radar Doppler spectrum. The cloud-only radar Doppler spectrum is symmetrical and near Gaussian (zero skewness; Kollias et al. 2011a) in uniform beamfilling conditions. Thus, the presence of small-sized drizzle results in positive skewness when downward Doppler velocities are positive in sign (e.g., Kollias et al. 2011a). A 1-day composite plot from marine stratus in the Azores exhibiting the relationship between Doppler spectra skewness and radar reflectivity is shown in Fig. 1a. A comprehensive interpretation of the observed relationship can be found in Kollias et al. (2011a). Here, we start at the conclusion of the authors' previous work: positive skewness at low radar reflectivities is a sensitive indicator of drizzle production through autoconversion. The skewness of the Doppler spectrum reverses sign at higher radar reflectivity values as drizzle comes to dominate the spectrum. Our spectrum decompositions are limited to

conditions for which skewness is sufficiently positive. Contours of frequency of occurrence of skewness by height from the cloud top for three different virga conditions [no virga (Fig. 1b), virga depth less than 200 m (Fig. 1c), and virga depth more than 200 m (Fig. 1d)] are shown in Fig. 1. The detection and determination of virga depth in marine stratocumulus clouds is based on the presence of radar echoes below the ceilometer-defined cloud base. Only radar observations above the ceilometer cloud bases have been used in Figs. 1b–d. In the absence of virga, in-cloud skewness is around zero throughout the cloud layer. In light virga conditions, the skewness has a positive bias in the upper three-quarters of the cloud layer and only near the cloud base does it reverse sign, indicating drizzle-dominated radar Doppler spectra. Deeper virga conditions are related to strong negative skewness values near the cloud base, indicating a more efficient accretion process and larger drizzle particles. In the following sections, we will present a method that uses the skewness behavior in liquid clouds to determine radar Doppler spectra suitable for decomposition.

a. Impact of radar signal characteristics and small-scale turbulence on radar Doppler spectra skewness

The mean skewness profile is a good indicator of drizzle particle growth processes in marine stratocumulus; however, the data shown in Figs. 1b–d exhibit considerable variability of the skewness values. The observed scatter in skewness values can compromise the use of a skewness threshold for the determination of radar Doppler spectra that contain small drizzle droplets. Thus, the first question to address is, what non-microphysical mechanisms are responsible for the observed variability in skewness? In the presence of purely homogeneous subvolume air dynamics, the cloud portion of the Doppler spectrum should be symmetric and very close to a Gaussian distribution (Kollias et al. 2011a). However, the estimation of the third moment of the radar Doppler spectrum is sensitive to the signal-to-noise ratio (SNR) and spectrum width σ_w conditions (Doviak and Zrnić 1993). To assess the “noisiness” of the skewness estimates, a large number of simulated Gaussian radar Doppler spectra were generated (Zrnić 1975) for a wide range of SNR and σ_w conditions (Fig. 2a). For each pair of SNR and σ_w conditions, 1000 simulated spectra were generated. Skewness values were determined using the same method applied to the recorded radar Doppler spectra and their standard deviation for each set of 1000 spectra was computed (plotted in Fig. 2a). The simulations exhibit that at SNR < 10 dB and spectrum width $\sigma_w < 0.1$ m s⁻¹, the skewness estimate is noisy. To assess the uncertainty of

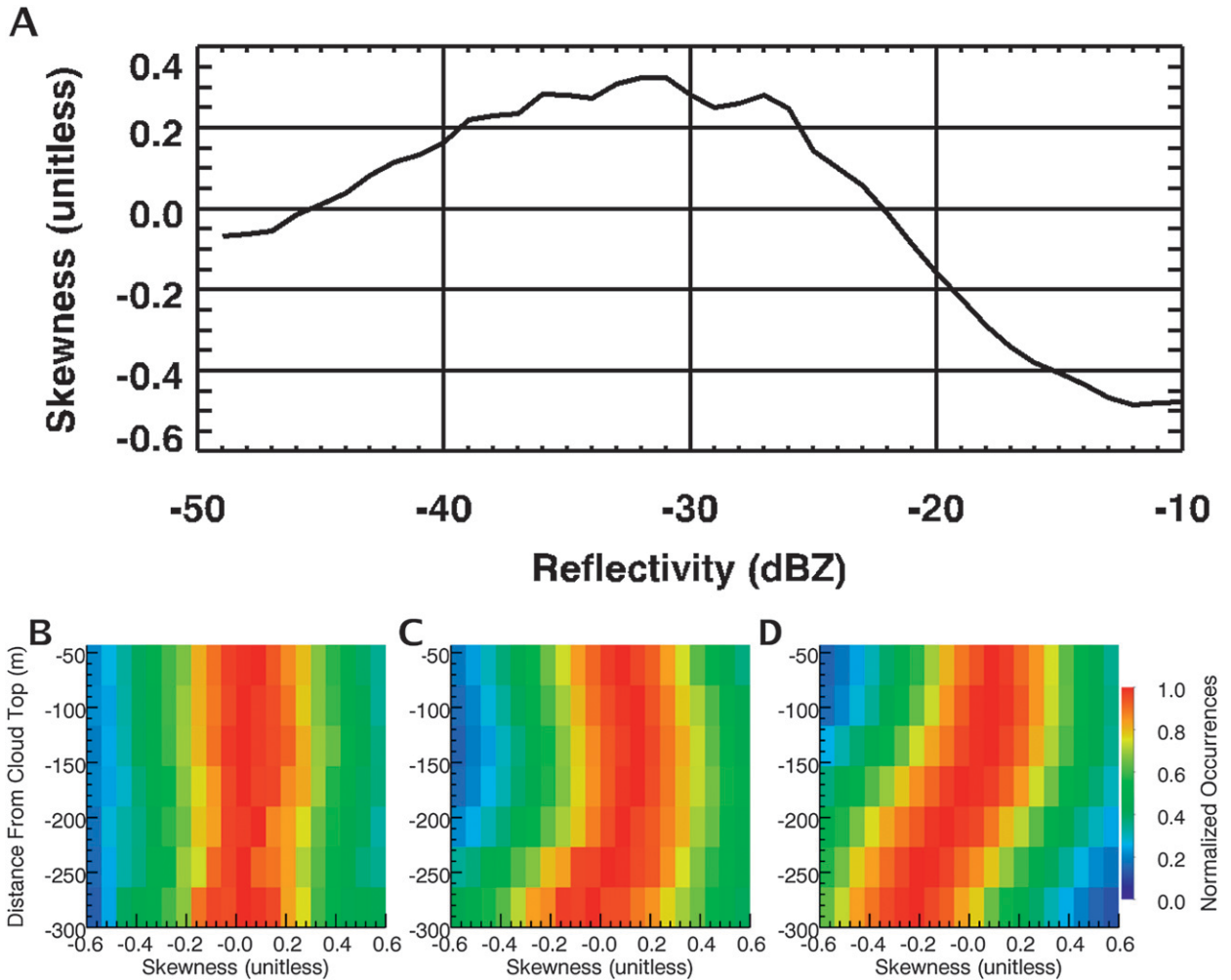


FIG. 1. (a) Relationship between mean radar Doppler spectrum skewness and radar reflectivity above CB using one day of observations of marine stratocumulus clouds during the AMF Azores deployment and contours of frequency of occurrence of skewness as a function of distance from the cloud top for three different virga depths: (b) no virga, (c) virga depth less than 200 m, and (d) virga depth more than 200 m. Data shown in (b)–(d) are from 27 days of stratocumulus observations.

skewness estimates from the recorded radar Doppler spectra, we need to map the observational dataset in the $\text{SNR}-\sigma_w$ parameter space. Figure 2b shows the distribution of the radar Doppler spectra from 27 days of stratocumulus observations in the $\text{SNR}-\sigma_w$ coordinate system. Only the $\text{SNR}-\sigma_w$ pairs of the radar Doppler spectra used in the proposed retrieval technique are reported in Fig. 2b. Thus, mapping the joint probability of $\text{SNR}-\sigma_w$ back to Fig. 2a enables a direct assessment of the expected uncertainty in skewness measurements. Typical cloud radar Doppler spectra have $\text{SNR} < 10$ dB; however, their spectrum width is higher than 0.1 m s^{-1} . Thus, a standard deviation of 0.1–0.25 in the skewness estimate should be anticipated in cloud conditions. This is consistent with the distribution of skewness values shown in Fig. 1.

Furthermore, inhomogeneous subvolume dynamics have the potential to lead to nonsymmetrical, skewed radar Doppler spectra (Fig. 3). Radar sampling volumes filled with small cloud droplets only (homogeneous reflectivity conditions) can lead to skewed or even bimodal radar Doppler spectra (e.g., Kollias et al. 2001) if sharp changes (horizontal or vertical) of the vertical air motion exist within the sampling volume. The subvolumes that experience different vertical air motion are “offset” with respect to each other in Doppler velocity. The scale of these dynamical structures is comparable to the sampling volume of the cloud radars (including the horizontal advection due to the signal integration time) at the level of observations (10–30 m horizontal extent). Such high-frequency (small scale) dynamics are often observed in boundary

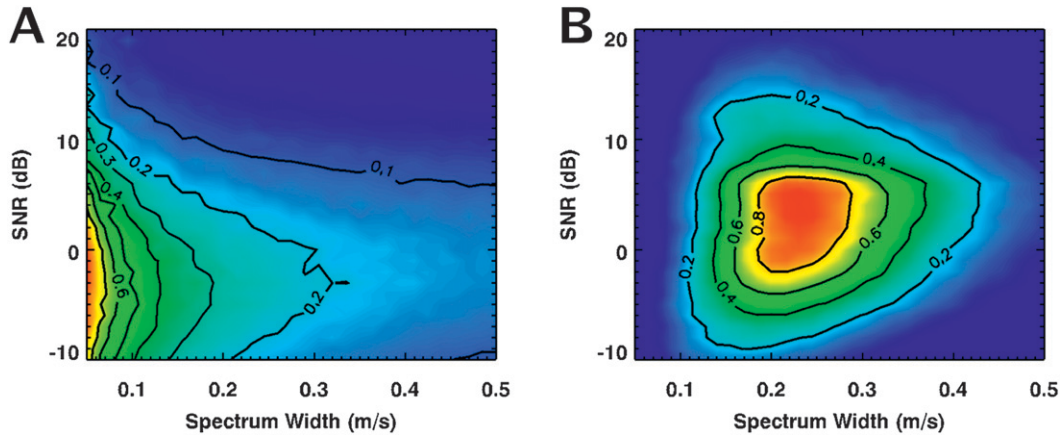


FIG. 2. (a) Estimates of the Doppler spectra skewness standard deviation for a wide range of SNR and Doppler spectrum width conditions. Estimates are based on simulated Gaussian radar Doppler spectra (zero skewness). Simulated radar Doppler spectra have the Nyquist velocity, spectral velocity resolution, and number of spectral averages of the WACR during the Azores deployment. For each pair of SNR and spectrum width conditions, 1000 simulated radar Doppler spectra are generated and the standard deviation of their skewness is estimated. (b) Distribution of the SNR and Doppler spectrum width of all the radar Doppler spectra from 27 days of stratocumulus where the retrieval was applied.

layer clouds as part of coherent eddies that are responsible for most of the turbulent vertical transport (e.g., Kollias and Albrecht 2000). The introduction of shorter signal integration in the ARM vertically pointing cloud radars (Kollias et al. 2007) significantly reduces, but

does not eliminate, the impact of small-scale dynamics on the shape of the radar Doppler spectrum. On the other hand, low-frequency (larger scale) dynamics result in an approximately linear gradient of the vertical air motion within the sampling volume, which can only lead to a

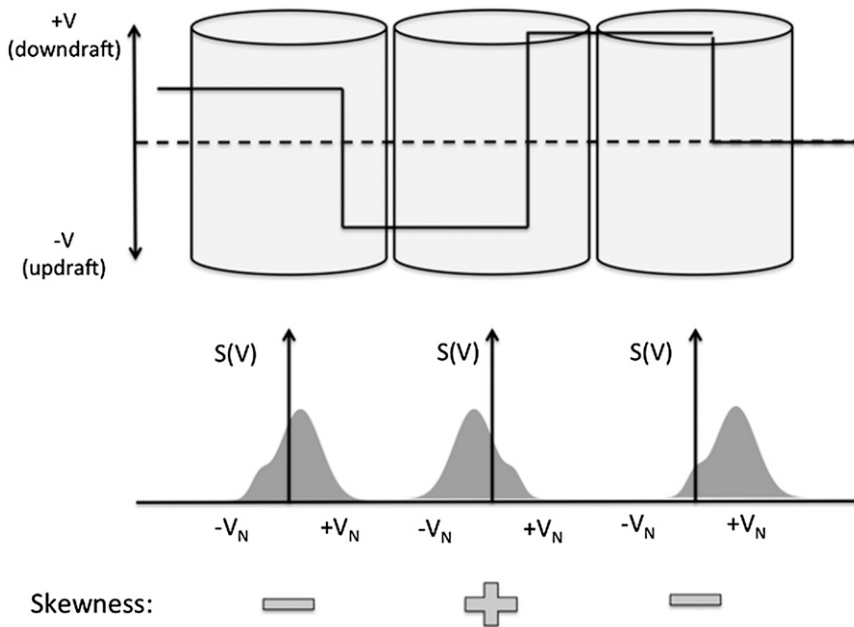


FIG. 3. Schematic representation of the dynamical mechanism that can result in non-symmetrical radar Doppler spectra despite homogeneous reflectivity conditions. (top) Three consecutive sampling volumes are shown, with the subsampling volume horizontal variability of the vertical air motion shown by the black line. (bottom) Corresponding resulting skewed radar Doppler spectra.

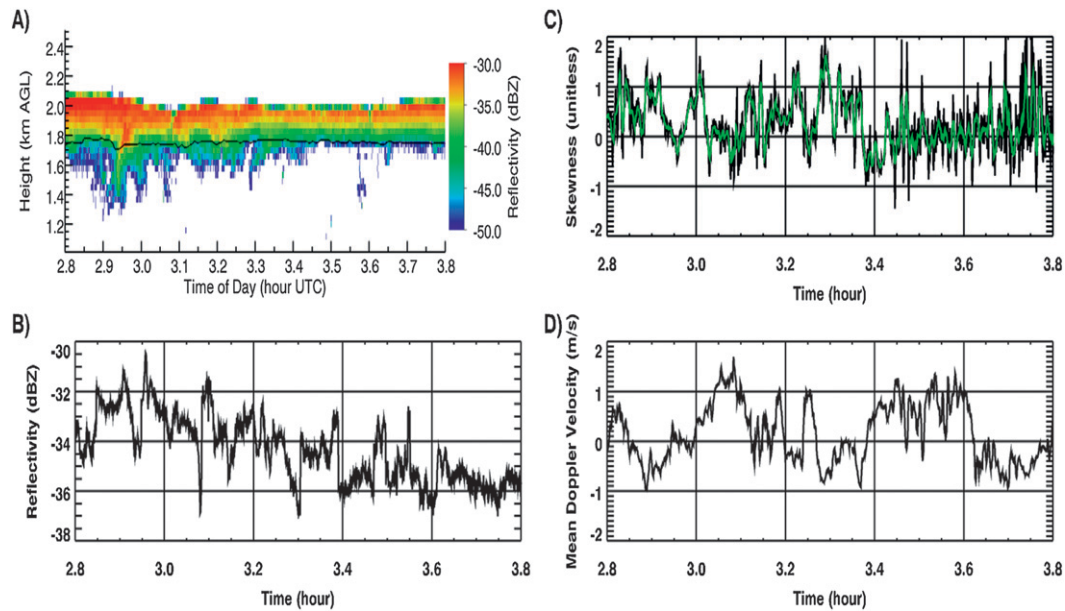


FIG. 4. (a) Time–height mapping of WACR radar reflectivity during a marine stratus event on 27 Jul 2010. Black line indicates the ceilometer CB, (b) time series of the WACR reflectivity at the middle of the cloud layer, (c) time series of the skewness of the radar Doppler spectrum at the middle of the cloud layer [raw measurements (black), 11-point running mean (green)], and (d) time series of the mean Doppler velocity at the middle of the cloud layer. All time series data were collected three range gates (129 m) above the CB height.

broadening of the radar Doppler spectrum (e.g., Doviak and Zrnić 1993).

The aforementioned effects—that is, the noisiness of the skewness estimate and the nonuniform dynamical beamfilling—introduce high-frequency variability in the skewness. This variability is manifested by magnitude and sign changes in the skewness of the radar Doppler spectra from one profile to another at the same height. Thus, the next question to address is, what are the magnitude and scales of the skewness signal induced by the microphysical mechanism (drizzle onset)? A careful look at the cloud-scale variability of skewness and dynamics can provide clues about the differences between the high-frequency terms and the microphysical impact on the skewness of the radar Doppler spectrum (Fig. 4). A typical time–height mapping of radar reflectivity from the WACR in a marine stratus cloud is shown in Fig. 4a. The black line indicates the laser-defined cloud base. Despite the shallow nature of the cloud (less than 300 m thick), virga are observed below the cloud base during the earlier part of the observed period (2.8–3.4 UTC). The time series of the WACR reflectivity at the middle of the cloud exhibits very small reflectivity values (below -30 dBZ) and only a small increase (~ 2 – 3 dB) during the early virga period. For the same period, the skewness of the radar Doppler spectrum and the mean Doppler velocity at the middle of the cloud layer are shown in Figs. 4c,d. During the earlier part of the period (2.8–3.4 UTC),

the skewness is generally positive (indicating the presence of drizzle particles). This is consistent with the presence of virga and the small increase in the radar reflectivity, indicating that the drizzle contribution to the total WACR reflectivity is smaller than the background cloud reflectivity. During the latter part of the observing period, a wide (low frequency) downdraft coincides with near-zero skewness values. The low-frequency variability of drizzle onset generates a microphysically induced positive skewness, while the high-frequency terms (noisiness of the estimate and nonuniform beamfilling) add an overriding noisiness in skewness. A relationship between positive skewness (drizzle onset) and updraft is prominent throughout the WACR dataset collected in the Azores (see Fig. 10).

Detailed inspection of the recorded WACR Doppler spectra provides additional insights into the scales of skewness variability induced by microphysics and high-frequency terms. In Fig. 5, the contours indicate the power spectral density (dB), the highest (red) corresponds to the dominant cloud peak and the lowest (blue) indicates the noise floor. These define the boundaries of the significant hydrometeor detections. The skewness is shown in white and the mean Doppler velocity in black (negative indicates updraft). All the WACR Doppler spectra have been recorded at the same height over the time period. The 8-min-long updraft coincides with persistent positive skewness values (Fig. 5a). Evidence of

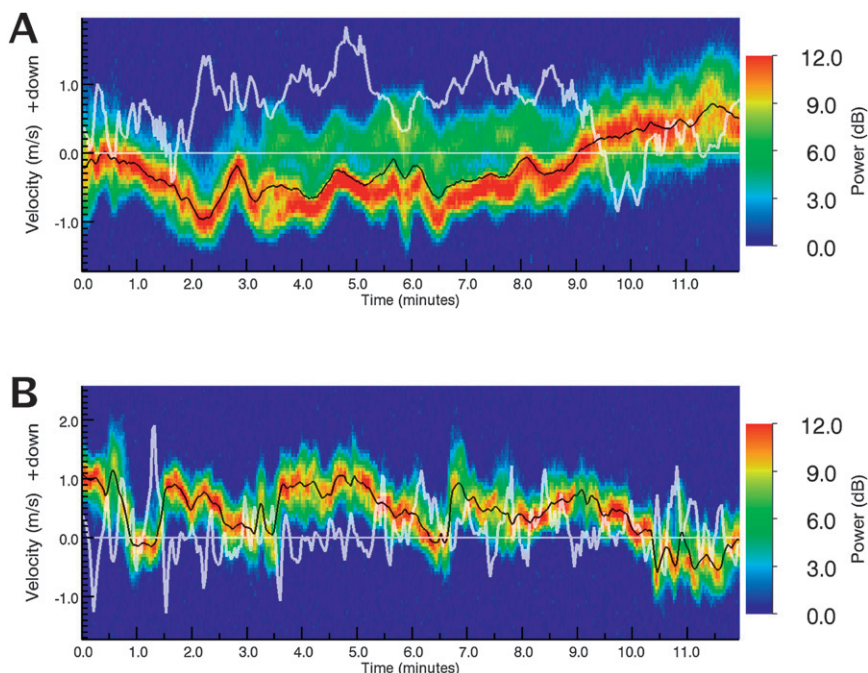


FIG. 5. Time series of WACR Doppler spectra collected at a constant height. Contours indicate the power (dB), the highest (red) corresponding to the dominant cloud peak and the lowest (blue) indicating the noise floor, which together define the boundaries of the significant hydrometeor detections. Skewness is shown in white and the mean Doppler velocity in black (negative indicates updraft). (a) Data were collected on 27 Jul 2010 at a height of 1913 m above the ground near the middle of the cloud layer and at a start time of 2.85 h UTC. (b) Data were collected on 27 Jul 2010 at a height of 1913 m above the ground near the middle of the cloud layer at a start time of 3.45 h UTC.

Doppler spectral broadening, including the presence of a second spectral peak, can be clearly seen within the updraft (minutes 3–9). In addition to the low-frequency skewness variability, there is an overriding high-frequency variability that can be attributed to either the noisiness of the skewness estimate or nonuniform beamfilling conditions (Fig. 4). Figure 5b provides a better illustration of the small-scale skewness variability induced by the high-frequency terms. The period is characterized by a wide downdraft and near-zero skewness values. Vertical shifts in the position of the cloud spectra peaks indicate the presence of small-scale turbulence that induces nonsymmetrical WACR Doppler spectra. The nonsymmetrical WACR Doppler spectra result in high-frequency changes in the sign of the skewness. The observed differences in the frequency and magnitude of the skewness changes induced by microphysics and the high-frequency terms are used in the separation algorithm described in the following section.

b. Decomposition of cloud and drizzle moments

Standard postprocessing is applied to the recorded WACR Doppler spectra composed of a series of

velocity bins (V_i , in m s^{-1}) having width ΔV (in m s^{-1}) and power spectral densities [P_i , in $\text{mm}^6 \text{m}^{-3} (\text{m s}^{-1})^{-1}$]. First, the Doppler spectrum noise floor P_N is objectively determined (Hildebrand and Sekhon 1974), as are the locations of left edge, right edge, and peak spectral power. The locations of any secondary maxima are determined, and according to whether any are found, the spectra are classified as unimodal or multimodal (Kollias et al. 2007). For each primary spectral peak, the first five moments are computed (reflectivity, mean Doppler velocity, spectrum width, skewness, and kurtosis) along with its SNR and spectral dynamic range (defined as the power difference between the maximum power spectral density within the peak and the noise floor spectral density). To reduce some of the inherent uncertainty in the radar Doppler spectra skewness (section 2a), a preprocessing step is performed in which a composite radar Doppler spectrum is estimated at a particular height above cloud base using a running window of consecutive radar profiles over a time interval of roughly 20-s duration. (Fig. 6a). When spectra are generated every 2.1 s (see Table 1), this window has nine profiles; for spectra generated every 4.2 s, it has five profiles. The composite

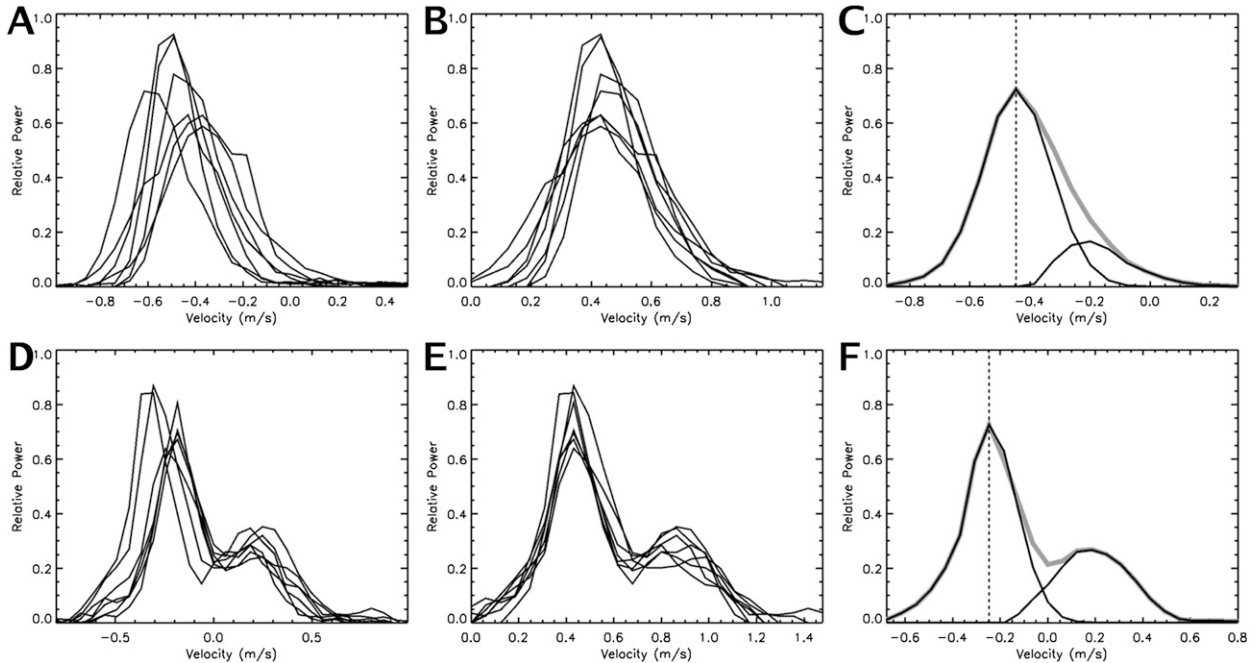


FIG. 6. (a) Nine consecutive radar spectra recorded at a common height above CB; (b) same spectra shifted in velocity such that their peaks coincide; and (c) bin-by-bin average of the shifted spectra (gray), retrieved cloud spectrum with Gaussian right portion (left black), and the retrieved drizzle spectrum generated by subtracting the cloud spectrum from the average spectrum (right black). (d)–(f) As in (a)–(c), but for a different set of spectra.

spectrum power spectral density is determined by generating shifted versions of any spectra in the window having a significant detection, such that all spectral peak power $P_{\text{peak},i}$ velocity positions $V_{\text{peak},i}$ coincide (Fig. 6b), and averaging the power spectral density at each bin (Fig. 6c). If half or more of the spectra in the window lack significant detections, processing does not continue for that set of spectra. Similar use of spectrum averaging to enhance information content of interest has been proposed in the past (e.g., Kollias et al. 2001; Giangrande et al. 2001). If we assume that the peak power position of each individual spectrum indicates the vertical air velocity, then we are in effect “tracking” the vertical air motion by shifting the spectra. It is apparent from Fig. 6a that if the consecutive radar Doppler spectra are not first shifted with respect to the cloud spectral peak, before averaging, then the resulting composite spectrum will be broader (emulating longer signal dwell effects; Kollias et al. 2007) and will distort the drizzle portion of the spectrum.

Once the composite (averaged) power spectrum is estimated (Fig. 6c), its skewness is computed. If it is found to be less than 0.1, then the ratio of drizzle to cloud reflectivity is designated to be unsuitably large or small, and no further processing is performed for this set of spectra. The next step is to compute the averaged vertical air motion $\langle w_{\text{air}} \rangle$ from the nine consecutive

radar Doppler spectra, estimated as the average of the velocity locations of the spectral density peaks, using

$$\langle W_{\text{air}} \rangle = \frac{\sum_{i=1,n} V_{\text{peak},i}}{n}, \quad (1)$$

where n is the number of spectra used to construct the composite spectrum and $V_{\text{peak},i}$ is the velocity location of the spectral density peaks $P_{\text{peak},i}$. The composite spectrum has no reference Doppler velocity coordinate, since the shifting of the original spectra to form the composite spectrum obscures the direct association of the composite spectrum’s velocity features, such as its peak position, with the velocity bins of the original spectra. The Doppler velocity coordinate of the composite spectrum is referenced by assigning the computed $\langle W_{\text{air}} \rangle$ to the velocity location of the composite spectrum’s peak power density.

Next, the power of the composite spectrum’s left half is computed using the following expression:

$$P_{\text{left}} = \sum_{i=1}^{m-1} p_i + \frac{p_m}{2}, \quad (2)$$

where m is the position of peak power density. Making the fundamental assumption that this power equals half

of the total cloud echo power, a doubling of this value leads to cloud reflectivity. Making the additional assumption, for now, that any significant drizzle echo power remains to the right of the composite spectrum's peak position, we construct an estimated right half of the cloud spectrum based on the left. As previously discussed, sources of variability cause the left half of the composite spectrum to depart from a Gaussian shape. However, the cloud reflectivity is conserved (depending only on the cloud particle distribution and the assumption of only incoherent scattering). To construct the right half of the cloud spectrum, we attribute to it the same amount of power as the left but recognize that we are not justified to assume that its *shape* is an actual mirror of the left half, we construct a *best estimate* by assuming a right half with a Gaussian shape (Fig. 6c), as follows:

$$p(i) = P_m e^{-(i-m)^2/2\sigma^2}, \quad i = m + 1, \dots, N, \quad (3)$$

where N is the number of elements in the composite spectrum, with maximum power density P_m , located at position m , and σ is calculated as follows:

$$\sigma = \frac{2 \sum_{i=0}^{m-1} P_i + P_m}{P_m \sqrt{2\pi}}. \quad (4)$$

The sigma used to construct the right half now leads immediately to a best estimate for σ_i :

$$\sigma_i = (dv)\sigma, \quad (5)$$

where dv is the difference in velocity between adjacent bins. After constructing a complete cloud spectrum in this way, a drizzle spectrum is generated by subtracting the cloud spectrum from the composite spectrum (Fig. 6c) as follows:

$$p_{\text{drizzle}}(i) = \begin{cases} p_i - p_{\text{cloud}_i} & \text{for } p_i \geq p_{\text{cloud}_i} \\ 0 & \text{for } p_i < p_{\text{cloud}_i} \end{cases}. \quad (6)$$

The drizzle reflectivity and reflectivity-weighted mean velocity are computed from the zeroth and first moments of the drizzle spectrum. The proposed decomposition technique assumes that the portion of the radar Doppler spectrum from the left edge to its peak is occupied only by cloud returns, and that any significant drizzle echo power remains to the right of the composite spectrum's peak position. This assumption becomes less valid with increasing turbulence and introduces a modest bias as a function of turbulence σ_r . Thus, once σ_r is retrieved,

TABLE 2. Dates from which data were used.

12 Aug 2009	10 Jun 2010
17 Sep 2009	11 Jun 2010
22 Nov 2009	13 Jun 2010
23 Nov 2009	14 Jun 2010
25 Nov 2009	16 Jun 2010
28 Nov 2009	22 Jun 2010
29 Nov 2009	29 Jun 2010
31 Jan 2010	6 Jul 2010
1 Feb 2010	27 Jul 2010
2 Apr 2010	29 Jul 2010
12 Apr 2010	31 Jul 2010
13 Apr 2010	8 Nov 2010
13 May 2010	11 Nov 2010
7 Jun 2010	

the drizzle reflectivity bias is estimated using the procedure described in the appendix and a correction is applied to both the retrieved cloud and drizzle radar reflectivity.

If the radar Doppler spectrum contains more than one distinct peak (Fig. 6d), then the same methodology is applied, although past studies have indicated that individual bimodal radar Doppler spectra can be directly decomposed (e.g., Shupe et al. 2004). Multimodal spectra can be generated by several mechanisms, based either in microphysics or dynamics (e.g., Kollias et al. 2001). Such conditions in liquid stratiform clouds include (i) a drizzle particle size distribution (PSD) that is lacking particles in the smallest size range, thus generating a size gap between cloud and drizzle droplets that is manifested as a velocity gap; and (ii) a sufficiently strong inhomogeneity in subvolume turbulence (Kollias et al. 2001). While the latter source of spectral multimodality is potentially problematic, the former is a great asset, generating what might be considered "golden" samples because of a distinct separation between cloud and drizzle peaks. Figure 6d shows a sequence of nine consecutive radar Doppler spectra, with several of them being clearly bimodal. Figure 6e shows the shifted radar Doppler spectra before averaging, and Fig. 6f shows the composite radar Doppler spectrum. Once again, the cloud peak is used to retrieve the vertical air motion and turbulence broadening, and the drizzle peak the drizzle moments.

3. Results

The AMF deployment in the Azores resulted in an extensive dataset of marine stratocumulus clouds from ground-based sensors. Twenty-seven days with solid marine stratocumulus conditions were selected for analysis from the 19-month-long dataset, as listed in Table 2. The WACR Doppler spectra dataset collected under

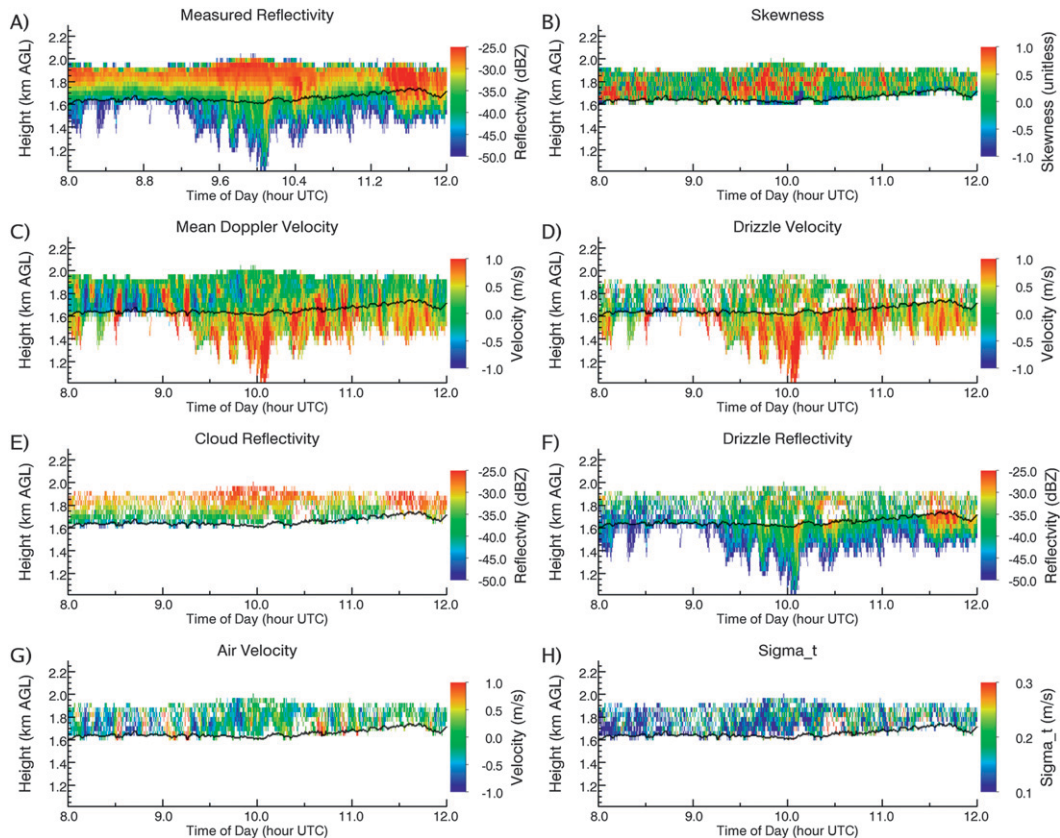


FIG. 7. On 27 Jul 2010, (a) measured reflectivity, (b) skewness of the composite spectra, (c) measured mean Doppler velocity, (d) retrieved reflectivity-weighted mean drizzle velocity above the ceilometer CB (black line) and measured mean Doppler velocity below CB, (e) retrieved cloud reflectivity, (f) retrieved drizzle reflectivity above the ceilometer CB (black line) and measured reflectivity below CB, (g) retrieved vertical air velocity, and (h) retrieved turbulence σ_t .

these conditions was analyzed using the procedure described in the previous section.

a. Time–height retrievals of cloud and drizzle moments

Retrievals from two short periods, one with light drizzle and one with moderate drizzle conditions, are presented to illustrate first, where the technique is applicable and second, the variability of the retrieved parameters in a time–height illustration (Figs. 7 and 8).

The 4-h-long light drizzle case exhibits a very stable cloud base at 1650 m and a cloud top between 1900 and 2000 m. Despite the low radar reflectivities observed throughout the cloud layer (below -30 dBZ), virga are observed below the cloud base as documented by the WACR echoes below the ceilometer-defined cloud base (Fig. 7a). Reflectivity generally increases with height in the cloud layer. This suggests that particle growth due to condensation dominates the observed radar reflectivity field. Thus, this case is ideal for applying the proposed

decomposition algorithm, and the overall positive Doppler spectra skewness values, especially during virga time periods (Fig. 7b), provide additional support. The observed mean Doppler velocity field exhibits significant discontinuity across the cloud base (Fig. 7c). In-cloud dynamics and the presence of cloud-scale eddies produce updraft and downdraft couplets visible during the nonprecipitating period (0815–0915 UTC). Below the cloud base, the magnitude of the downward mean Doppler velocities is higher than above the cloud base. This is attributed to the absence of updrafts, and the role of evaporation that modifies the drizzle size distribution and induces downdraft air motions. The retrieved cloud-only radar reflectivity is shown in Fig. 7e. Not surprisingly, it is very similar to the observed radar reflectivity, indicating that the cloud droplets dominate the observed radar reflectivity. The retrieved drizzle-only reflectivity-weighted mean velocity (including air motion) and drizzle-only reflectivity are shown in Figs. 7d and 7f. The retrieved vertical air motion (Fig. 7g) has been added to

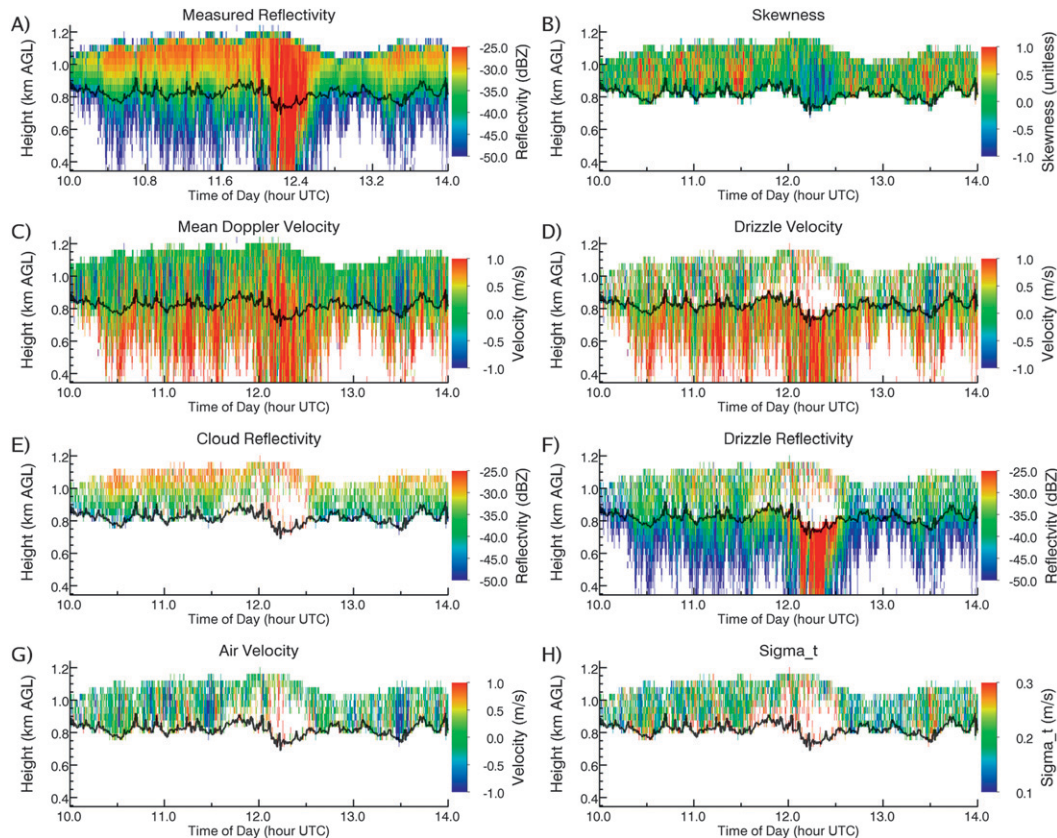


FIG. 8. As in Fig. 7, but for 8 Nov 2010. Area of pronounced negative skewness following 1200 UTC in (b) signals that the drizzle reflectivity has become too great with respect to cloud for spectrum decompositions to be performed.

the retrieved drizzle-only reflectivity-weighted mean fall speed to provide a consistent comparison of the velocities above and below the cloud base. The air motion retrievals (Figs. 7g,h) demonstrate several coherent drafts. The turbulence-induced spectral broadening σ_t parameter is directly related to the eddy dissipation rate (Kollias et al. 2001) and exhibits coherent structures within the cloud with values between 0.1 and 0.25 m s^{-1} . Below the cloud base, no retrieval is attempted; thus, the observed radar reflectivity and mean Doppler velocity are shown. The magnitude and structure of retrieved drizzle-only reflectivity-weighted mean velocities (including the vertical air motion) above the cloud base are consistent with the observed velocities below the cloud base. This correlation offers a qualitative validation for the ability of the retrieval technique to separate the radar Doppler moments of small drizzle particles. The retrieved drizzle reflectivities are also consistent with the magnitude of the drizzle reflectivities below the cloud base. There are a few areas in the cloud where no retrievals were performed (white gaps). These areas correspond to (i) areas with no drizzle droplets, (ii) areas with drizzle droplets below the sensitivity of the technique, or (iii) areas where the drizzle

signal is higher than the cloud signal and the decomposition is not possible without large uncertainty.

Retrievals from another 4-h-long period with moderate drizzle are shown in Fig. 8. The cloud-top height is at 1100–1200 m, and the cloud base height is variable from 800 to 900 m. Stronger WACR reflectivities are observed in this case (up to -20 dBZ), with the higher reflectivities found near the upper part of the cloud; however, several streaks of high radar reflectivity are observed, indicating large drizzle particles (1215–1230 UTC). The Doppler spectra skewness (Fig. 8b) exhibits pockets of positive values that coincide with weak drizzle below the cloud base and an area of negative skewness that coincides with the strongest drizzle cluster (1215–1230 UTC). Negative radar Doppler spectra skewness and high radar reflectivities indicate growth of the drizzle spectral peak due to collection dominating the radar Doppler spectrum (Kollias et al. 2011b). The proposed retrieval technique is not applicable in areas with negative skewness (white gaps). The mean Doppler velocity (Fig. 8c) indicates the presence of radar volumes with upward and downward Doppler velocities within the cloud. The retrieved cloud-only reflectivities (where performed) are higher near the

cloud top (Fig. 8e). The retrieved drizzle-only reflectivity-weighted mean velocity (including vertical air motion) and drizzle-only reflectivity are shown in Figs. 8d and 8f. The retrieved vertical air motion (Fig. 8g) has been added to the retrieved drizzle-only reflectivity-weighted mean fall speed to provide consistent comparison of the velocities above and below the cloud base. The turbulence-induced spectral broadening σ_t parameter exhibits higher values ($0.15\text{--}0.3\text{ m s}^{-1}$) in this case. Below the cloud base, no retrieval is attempted; thus, the observed radar reflectivity and mean Doppler velocity are shown. The magnitude and structure of retrieved drizzle-only reflectivity-weighted mean velocities above the cloud base are consistent with the observed velocities below the cloud base. The magnitudes of the retrieved vertical air motions are within $\pm 0.5\text{ m s}^{-1}$, with no apparent bias introduced by the drizzle particles (not shown here).

b. Statistics of cloud and drizzle radar Doppler moments

The decomposition of cloud and drizzle moments can lead to valuable statistics when a large dataset is available. Using all WACR Doppler spectra from the 27 days of solid stratocumulus conditions that satisfy the skewness requirement, statistics of retrieved cloud and drizzle radar Doppler moments are compiled. First, the applicability of the proposed spectra decomposition technique, defined as the fraction of WACR Doppler spectra that qualified for cloud and drizzle spectral decompositions as a function of height below the cloud top, is shown in Fig. 9. At each height below the cloud top, the fraction of significant detections (gates with a valid reflectivity) having successful retrievals from 27 days of stratocumulus clouds is shown. The fraction is at minimum near the cloud base (15%) and maximum near the cloud top (45%). The maximum applicability of the technique near the cloud top is consistent with the presence of higher cloud radar reflectivities near the top that enable drizzle retrievals over a larger range of radar reflectivities. The challenge of applying the technique near the cloud base is attributable to two factors: smaller cloud-only radar reflectivity and drizzle growth due to collection toward the cloud base. These two factors limit the availability of radar detections having cloud-radar reflectivity higher than the drizzle-radar reflectivity.

The relationship between the retrieved vertical air motion and the radar Doppler spectrum skewness from all 27 days of stratocumulus conditions is shown in Fig. 10a. This relationship demonstrates the tendency for positive skewness values to occur in updrafts. However, the technique is not limited to only updrafts, since there is a significant fraction of decomposed Doppler spectra with downward air motion (see Fig. 11). Another

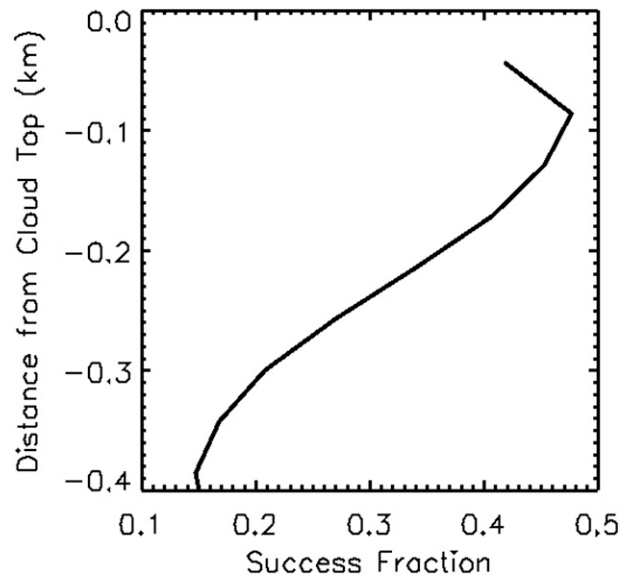


FIG. 9. For 27 stratocumulus days, fraction of recorded spectra having successful retrievals at the indicated heights below cloud top.

interesting observation is that the distribution of skewness values falls below 0.1, the acceptance threshold that is applied for the composite spectrum (Fig. 10b). However, the reported skewness values in Fig. 10a are from all individual radar Doppler spectra used in generating spectra composites. This underscores the importance of averaging consecutive radar Doppler spectra to remove the inherent noisiness of the skewness estimator and to remove wind shear effects.

The probability distributions of vertical air velocity, reflectivity-weighted mean drizzle velocity, and reflectivity-weighted mean drizzle fall speed for all retrievals during the 27 days of stratocumulus are shown in Fig. 11. The vertical air motion distribution is centered near zero, indicating that almost half of the spectral decompositions were performed in downdrafts; however, updrafts are associated with higher positive values of skewness (Fig. 10a). The drizzle PSD reflectivity-weighted mean fall speed is centered at 0.25 m s^{-1} with a spread of 0.2 m s^{-1} (Fig. 11). On average, these values correspond to small drizzle droplets with diameters between 20 and $60\ \mu\text{m}$. This is consistent with the expectation that the new proposed algorithm is suitable to retrieve drizzle radar moments at early stages of drizzle production. Finally, the retrieved drizzle PSD reflectivity-weighted mean velocity (including retrieved vertical air motion) is wider, indicating the role of vertical air motion in accelerating or slowing down drizzle particle sedimentation. However, the majority of the retrieved drizzle particles found in updrafts continue to fall, indicating drizzle-sorting effects.

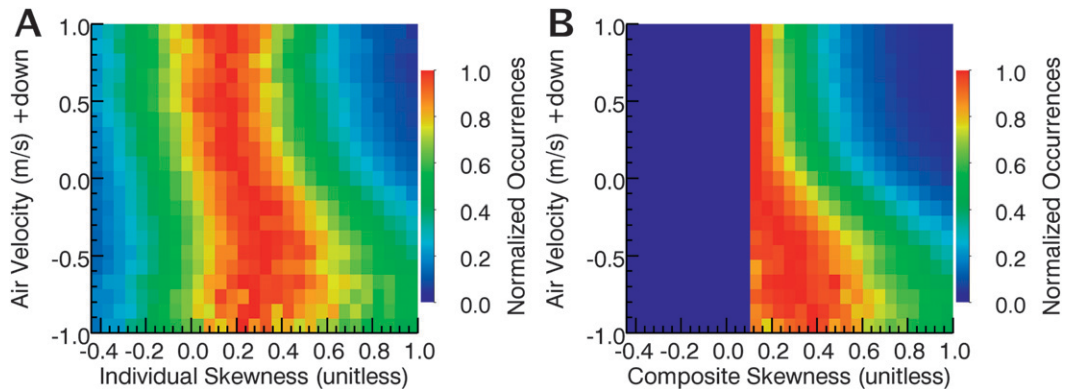


FIG. 10. Relative frequency of occurrence of radar Doppler spectra skewness as a function of the retrieved vertical air velocity from all 27 stratocumulus days. Positive velocities are downward. (a) Data are from all individual radar Doppler spectra occurring within cloud, i.e., all spectra used to construct composite spectra. (b) Data are from all composite spectra deemed satisfactory for spectrum decomposition.

c. Statistical comparison of drizzle reflectivities above and below the cloud base

A key component of every retrieval algorithm is validation of the retrieved parameters using independent measurements. The lack of aircraft measurements during the Azores field campaign prevents validation of the retrievals using in situ microphysical and dynamical measurements. To partially compensate for this, the cloud base (CB) height is used as a natural boundary between WACR observations of clouds with embedded drizzle (above the cloud base) and drizzle-only observations (below the cloud base). Comparisons can then be made between members of these two groups. In particular, we are interested to compare the values of drizzle reflectivity retrieved just above the cloud base (at range gate CB+1) with the drizzle reflectivity observed just below cloud base (at range gate CB-1). We disqualify from these comparisons the range gate located at cloud base due to incomplete beamfilling by cloud particles.

Figure 12a shows a scatterplot comparing retrieved drizzle reflectivity at CB+1 on the horizontal axis with measured drizzle reflectivity at CB-1 on the vertical axis. The plots present all data from 27 days; the mean bias of the retrievals within the range of the plot is -1.7 dBZ. Figure 12b compares retrieved drizzle reflectivity-weighted mean velocity at CB+1 with measured drizzle mean Doppler velocity at CB-1; the mean bias for these retrievals is 5 cm s^{-1} . Very good consistency above and below cloud base is observed for both reflectivity and velocity.

4. Summary

The decomposition of cloud and drizzle radar moments is the first step toward cloud, drizzle, and turbulence

retrievals that can provide important information about the interaction of microphysics and dynamics at cloud scale. Previous efforts have focused on the exploitation of either drizzle-free (e.g., Kollias et al. 2001) or drizzle-dominated (e.g., Frisch et al. 1995) radar returns. Here, a new Doppler spectrum-based decomposition approach is proposed that fills the void in decomposing cloud and drizzle radar moments when cloud radar reflectivity dominates (early drizzle onset regime). The technique is based on the Gaussian shape of the cloud-only radar Doppler spectrum (zero skewness) due to turbulence, with small amounts of drizzle only adding a small asymmetry and creating a positively skewed spectrum. A Gaussian fit is used to construct an estimated cloud-only component spectrum, and by subtraction from the observed spectrum, an estimated drizzle-only spectrum. Once separated, the cloud spectral peak can be

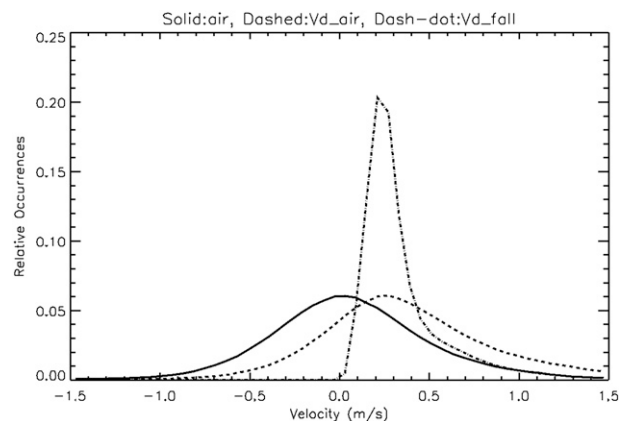


FIG. 11. For all retrievals during 27 stratocumulus days, the probability distributions of vertical air velocity (solid), reflectivity-weighted mean drizzle velocity (dashed), and reflectivity-weighted mean drizzle fall speed (dashed-dotted).

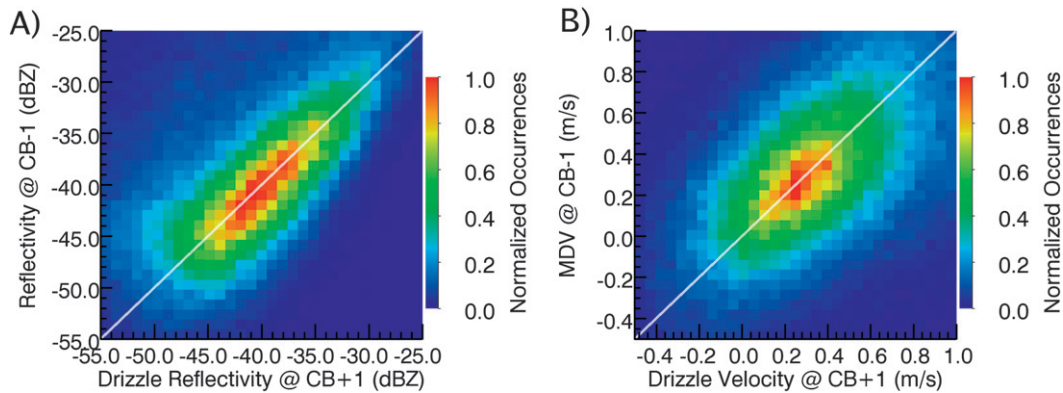


FIG. 12. For all retrievals from 27 days, scatterplots of (a) retrieved drizzle reflectivity one range gate above CB (42.86 m, and called CB+1) vs measured drizzle reflectivity one range gate below cloud base, and (b) retrieved drizzle reflectivity-weighted mean velocity (which includes air motion) one range gate above CB vs measured drizzle mean Doppler velocity one range gate below CB (CB-1).

used to retrieve vertical air motion and eddy dissipation rates. The drizzle spectral peak can be used to estimate the three radar moments of the drizzle particle size distribution.

The radar Doppler spectrum decomposition technique was applied to a large dataset collected in the Azores during the ARM Mobile Facility deployment there. The retrieved drizzle-only radar moments (reflectivity and reflectivity-weighted mean drizzle velocity with air motion) above the cloud base are coherent in time and height, and agree very well with the observed drizzle moments below the cloud base. Furthermore, the distribution of retrieved vertical air motion from all 27 days reveals that the decomposition technique was almost equally applied to updraft and downdraft conditions. Small drizzle droplets (20–60 μm in diameter) are consistently found in updrafts of 0.1–0.3 m s^{-1} , and in the majority of the observations the drizzle particles continue to fall, rather than being carried upward by the updrafts.

The cloud base is a natural boundary for radar Doppler spectra that contain a mixture of cloud and drizzle particles above the cloud base and only drizzle particles below the cloud base. The distributions of the retrieved drizzle-only radar reflectivities above the cloud base and observed reflectivities below the cloud base agree very well. This validation of drizzle retrievals across the cloud base adds confidence to the proposed retrieval technique.

On average, 15% (near the cloud base) to 45% (near the cloud top) of the recorded radar Doppler spectra observed in the Azores satisfied the conditions for applying the decomposition technique. This is a significant portion of the overall ground-based radar observations and fills a regime where existing techniques are not

applicable. The retrieval algorithm has the potential to characterize the dynamical and microphysical conditions at cloud-scale during the transition from cloud to precipitation and thus has significant implications for improving our understanding of the conditions involving drizzle onset in liquid clouds. The proposed separation framework could be applicable to other challenging conditions, such as mixed-phase clouds. Furthermore, the recent announcement from the U.S. DOE ARM program for the installation of a fixed ARM site in the Azores makes this work relevant for future retrievals using the long-term dataset that will be produced there.

Acknowledgements. This research was supported under Contract DE-AC02-98CH10886 by the Atmospheric System Research program of the Office of Biological and Environmental Research of the U.S. Department of Energy. Data were obtained from the ARM Climate Research Facility of the U.S. Department of Energy.

APPENDIX

Drizzle Bias Estimation due to Turbulence

The proposed decomposition technique is based on the assumption of an on-average symmetrical cloud-only radar Doppler spectrum and the absence of drizzle returns in the Doppler velocity bins between the left edge and the spectral peak of the observed radar Doppler spectrum. At low-turbulence conditions ($\sigma_t \leq 0.1 \text{ m s}^{-1}$), this is a good assumption. However, as turbulence increases, infiltration of drizzle echo power into the left half of the cloud power spectrum increases and this induces an overestimation of the cloud radar reflectivity and an underestimation of the drizzle radar

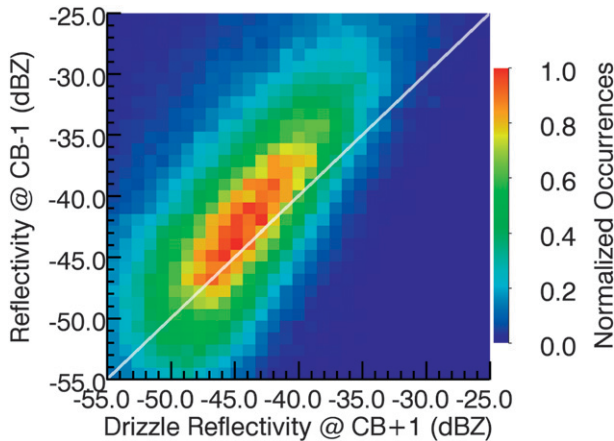


FIG. A1. Reflectivity measured one radar range gate below the CB (42.86 m) vs drizzle reflectivity retrieved one radar range gate above the CB without applying a compensation factor for turbulence over 27 days.

reflectivity. This behavior is reproducible in radar Doppler spectra simulations. Here, we estimate the induced bias as a function of turbulence. Figure A1 shows drizzle reflectivity retrieved at one range gate above cloud base plotted against drizzle reflectivity measured at one range gate below cloud base. Assuming that on a statistical basis, the retrieved (CB+1) and observed (CB−1) drizzle radar reflectivity should agree very well, the observed offset from the white 1:1 line indicates a negative bias in retrieved drizzle reflectivity. This bias is explained by drizzle echo power entering the left half the cloud spectrum and being incorrectly attributed to cloud rather than drizzle.

To demonstrate the control that turbulence has on this negative bias, we bin retrieved drizzle reflectivity values according to retrieved σ_r and plot mean bin reflectivity versus σ_r in Fig. A2. The relationship is seen to be nearly linear, revealing a simple σ_r -based correction factor, Z' , that can substantially reduce the retrieval bias, as shown:

$$Z' = 50(\sigma_t - 5).$$

Comparison of Fig. A1 with Fig. 12a shows the benefit of applying this correction factor. Next, we describe how the process of decomposing spectra into cloud and drizzle partitions is modified to incorporate this correction factor.

As already described, after initial conditioning and screening, a spectrum left half is identified and attributed to half of the cloud reflectivity. This spectrum left half is also attributed to half of the turbulent broadening, σ_t . A complete cloud spectrum is formed by reflecting the area under the spectrum left half about its right edge. The drizzle reflectivity is determined to be

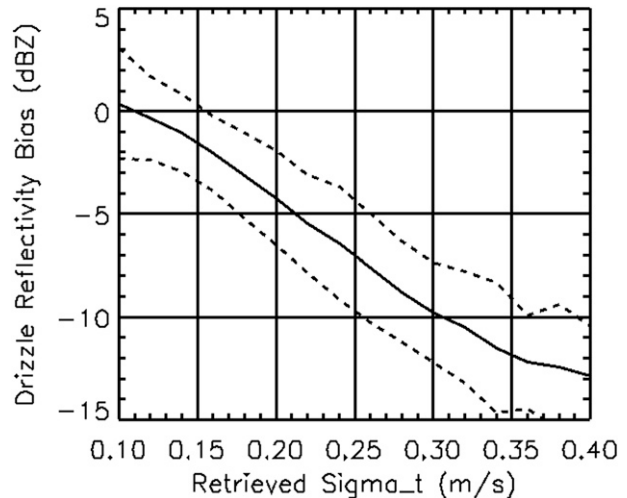


FIG. A2. For 27 days, solid curve shows the bias of retrieved drizzle reflectivity one range gate above CB (42.86 m) vs σ_r . Reference for the bias is the measured reflectivity one range gate below the CB; dashed curves show the standard deviation of the bias daily means.

the difference between total reflectivity and total cloud reflectivity.

At this point we introduce the turbulence-based compensation factor Z' by using it to scale the retrieved drizzle reflectivity, as shown:

$$Z'_{\text{drizzle}} = Z_{\text{drizzle}} + Z'$$

Subtraction of the new drizzle reflectivity, Z'_{drizzle} , from the total leads to a corrected (and reduced) cloud reflectivity. The height of the cloud spectrum is scaled by the fractional reduction of cloud reflectivity. From here, the remainder of the decomposition process proceeds as originally described.

REFERENCES

- Atlas, D., R. S. Srivastava, and R. S. Sekhon, 1973: Doppler radar characteristics of precipitation at vertical incidence. *Rev. Geophys. Space Phys.*, **11**, 1–35.
- Babb, D. M., J. Verlinde, and B. A. Albrecht, 1999: Retrieval of cloud microphysical parameters from 94-GHz radar Doppler power spectra. *J. Atmos. Oceanic Technol.*, **16**, 489–503.
- Battan, L. J., 1964: Some observations of vertical velocities and precipitation sizes in a thunderstorm. *J. Appl. Meteor.*, **3**, 415–420.
- Brenguier, J. L., and R. Wood, 2009: Observational strategies from the micro to meso scale. *Clouds in the Perturbed Climate System: Their Relationship to Energy Balance, Atmospheric Dynamics, and Precipitation*, J. Heintzenberg and R. J. Charlson, Eds., MIT Press, 487–510.
- Delanoë, J., A. Protat, D. Bouniol, A. Heymsfield, A. Bansemmer, and P. Brown, 2007: The characterization of ice cloud properties from Doppler radar measurements. *J. Appl. Meteor. Climatol.*, **46**, 1682–1698.

- Deng, M., and G. G. Mace, 2006: Cirrus microphysical properties and air motion statistics using cloud radar Doppler moments. Part I: Algorithm description. *J. Appl. Meteor. Climatol.*, **45**, 1690–1709.
- Doviak, R., and D. Zrnić, 1993: *Doppler Radar and Weather Observations*. 2nd ed. Academic Press, 458 pp.
- Frisch, A. S., C. W. Fairall, and J. B. Snider, 1995: Measurement of stratus cloud and drizzle parameters in ASTEX with a K_a-band Doppler radar and microwave radiometer. *J. Atmos. Sci.*, **52**, 2788–2799.
- Giangrande, S. E., D. M. Babb, and J. Verlinde, 2001: Processing millimeter wave profiler radar spectra. *J. Atmos. Oceanic Technol.*, **18**, 1577–1583.
- , E. P. Luke, and P. Kollias, 2010: Automated retrievals of precipitation parameters using non-Rayleigh scattering at 95 GHz. *J. Atmos. Oceanic Technol.*, **27**, 1490–1503.
- Gossard, E. E., 1994: Measurements of cloud droplet size spectra by Doppler radar. *J. Atmos. Oceanic Technol.*, **11**, 712–726.
- , J. B. Snider, E. E. Clothiaux, B. Martner, J. S. Gibson, R. A. Kropfli, and A. S. Frisch, 1997: The potential of 8-mm radars for remotely sensing cloud drop size distributions. *J. Atmos. Oceanic Technol.*, **14**, 76–87.
- Hauser, D., and P. Amayenc, 1981: A new method for deducing hydrometeor-size distributions and vertical air motions from Doppler radar measurements at vertical incidence. *J. Appl. Meteor.*, **20**, 547–555.
- Hildebrand, P. H., and R. S. Sekhon, 1974: Objective determination of the noise level in Doppler spectra. *J. Appl. Meteor.*, **13**, 808–811.
- Kollias, P., and B. A. Albrecht, 2000: The turbulence structure in a continental stratocumulus cloud from millimeter wavelength radar observations. *J. Atmos. Sci.*, **57**, 2417–2434.
- , —, R. Lhermitte, and A. Savtchenko, 2001: Radar observations of updrafts, downdrafts, and turbulence in fair-weather cumuli. *J. Atmos. Sci.*, **58**, 1750–1766.
- , —, and F. D. Marks Jr., 2002: Why Mie? Accurate observations of vertical air velocities and rain drops using a cloud radar. *Bull. Amer. Meteor. Soc.*, **83**, 1471–1483.
- , E. E. Clothiaux, M. A. Miller, B. A. Albrecht, G. L. Stephens, and T. P. Ackerman, 2007: Millimeter-wavelength radars: New frontier in atmospheric cloud and precipitation research. *Bull. Amer. Meteor. Soc.*, **88**, 1608–1624.
- , J. Remillard, E. Luke, and W. Szyrmer, 2011a: Cloud radar Doppler spectra in drizzling stratiform clouds: 1. Forward modeling and remote sensing applications. *J. Geophys. Res.*, **116**, D13201, doi:10.1029/2010JD015237.
- , W. Szyrmer, J. Remillard, and E. Luke, 2011b: Cloud radar Doppler spectra in drizzling stratiform clouds: 2. Observations and microphysical modeling of drizzle evolution. *J. Geophys. Res.*, **116**, D13203, doi:10.1029/2010JD015238.
- Lhermitte, R., 1988: Observations of rain at vertical incidence with a 94 GHz doppler radar: An insight on Mie scattering. *Geophys. Res. Lett.*, **15**, 1125–1128.
- Luke, E. P., P. Kollias, and M. D. Shupe, 2010: Detection of super-cooled liquid in mixed-phase clouds using radar Doppler spectra. *J. Geophys. Res.*, **115**, D19201, doi:10.1029/2009JD012884.
- Rogers, R. R., and R. J. Pilić, 1962: Radar measurements of drop-size distributions. *J. Atmos. Sci.*, **19**, 503–506.
- , W. L. Ecklund, D. A. Carter, K. S. Gage, and S. A. Ethier, 1993: Research applications of a boundary-layer wind profiler. *Bull. Amer. Meteor. Soc.*, **74**, 567–580.
- Shupe, M. D., P. Kollias, S. Y. Matrosov, and T. L. Schneider, 2004: Deriving mixed-phase cloud properties from Doppler radar spectra. *J. Atmos. Oceanic Technol.*, **21**, 660–670.
- Wakasugi, K., A. Mizutani, M. Matsuo, S. Fukao, and S. Kato, 1986: A direct method for deriving drop-size distribution and vertical air velocities from VHF Doppler radar spectra. *J. Atmos. Oceanic Technol.*, **3**, 623–629.
- Williams, C. R., W. L. Ecklund, and K. S. Gage, 1995: Classification of precipitating clouds in the tropics using 915-MHz wind profilers. *J. Atmos. Oceanic Technol.*, **12**, 996–1012.
- , —, P. E. Johnston, and K. S. Gage, 2000: Cluster analysis techniques to separate air motion and hydrometeors in vertical incident profiler observations. *J. Atmos. Oceanic Technol.*, **17**, 949–962.
- Zrnić, D. S., 1975: Simulation of weatherlike Doppler spectra and signals. *J. Appl. Meteor.*, **14**, 619–620.